

## Modal Focusing Effect of Positive and Negative Ions by a Three-Dimensional Plasma-Sheath Lens

E. Stamate and H. Sugai

*Department of Electrical Engineering and Computer Science, Nagoya University, Furo-cho, Chikusa-ku, Nagoya 464-8603, Japan*  
(Received 20 December 2004; published 1 April 2005)

A complex focusing effect of positive and negative ions caused by the sheath forming to biased electrodes that interface insulators has been found by solving in three dimensions the potential distribution and ion kinetics within the sheath. Thus, intrinsically correlated with the sheath shape, certain electrical charges are focused on the surface, forming well defined patterns named modal lines and modal spots. Their superposition to the previously reported discrete focusing leads to a total flux that represents a “fingerprint” of the entire sheath on the electrode surface. The ion flux pattern is developed experimentally on the surface of square and octagonal electrodes exposed to Ar/SF<sub>6</sub> and CF<sub>4</sub> plasmas. Present results are of high potential importance for fundamental studies concerning sheath formation and charge kinetics and also in a wide range of plasma applications.

DOI: 10.1103/PhysRevLett.94.125004

PACS numbers: 52.25.-b, 52.27.-h

The sheath is a space charge layer that forms to an electrode whenever its potential  $V_0$  is different than the plasma potential  $V_{pl}$  [1]. Despite the extensive theoretical coverage, basic concepts of the sheath such as the pre-sheath and the sheath edge are still under debate [2–6]. So far, most of these investigations have been done in one dimension, but recent trends in plasma processing, including anisotropic etching or ion implantation, have attracted much attention towards two- or three-dimensional approaches [7–11]. In fact, whatever the application would be, the correct description of the sheath surrounding electrodes of finite sizes immersed in laboratory produced plasmas is of critical importance in particle and energy balance, charge kinetics, ion flux distribution, surface modification, discharge stability, etc. Following our interest in negative ion detection by Langmuir probes we recently reported experimental evidence of the discrete-focusing effect of ions for biased planar probes including the formation of a passive surface (PS) of no ion impact at the edge and a nonuniformly bombarded active surface (AS) at the center [12,13]. Based on this effect, a sheath-lens probe for negative ion detection has been developed [13].

In this Letter we are reporting the existence of an additional focusing effect, subsequently named modal focusing, that is formed by a certain group of charged particles accelerated through the potential distribution of the sheath surrounding plane electrodes that interface insulators.

Let us suppose a plane electrode of surface  $S_e$  and biased at potential  $V_0 \neq V_{pl}$  that comes in contact with an insulator. The potential distribution in the sheath,  $V(x, y, z)$ , is given by the following Poisson equation:

$$\nabla^2 V(x, y, z) = -\frac{e}{\epsilon_0} [\pm n_i^*(V) \mp (n_e^*(V) + n_{ni}^*(V))], \quad (1)$$

where upper signs stand for  $V_0 < V_{pl}$  (positive sheath) and lower signs for  $V_0 > V_{pl}$  (negative sheath) and  $n_i^*(V)$ ,

$n_e^*(V)$ , and  $n_{ni}^*(V)$  are the positive ion, electron, and negative ion density distributions in the sheath, respectively. In order to solve Eq. (1) we can assume a Boltzmann distribution for electrons and negative ions, and positive ions governed by momentum and energy conservation for  $V_0 < V_{pl}$ . For  $V_0 > V_{pl}$  we can consider Boltzmann distributed positive ions with electrons and negative ions entering the sheath with thermal velocities,  $v_{e,ni}^{th} = (8kT_{e,ni}/\pi m_{e,ni})^{1/2}$ , where  $T_e$  and  $T_{ni}$  are the electron and negative ion temperatures. If  $V = \text{const}$  is an equipotential surface of area  $S$  in the sheath, then  $V_{sh} = kT_e/2$  is defining, according to the Bohm criterion for  $V_0 < V_{pl}$  and  $n_{ni} = 0$ , the sheath edge of surface  $S_{sh}$ . For charges that follow the continuity equation in the sheath ( $n_i^*$  for  $V_0 < V_{pl}$  and  $n_{e,ni}^*$  for  $V_0 > V_{pl}$ ), one should specify  $S(V)$ , a problem that has been described in detail elsewhere [13]. Equation (1) was solved using the finite element method for planar electrodes of square and octagonal shapes with the  $z$  axis perpendicular to the conducting surface and  $-z$  facing the insulated side. For simplicity, since  $|V_0| \gg V_{pl}$ , the potential of the insulated surface (the electrode's back side) was set to plasma potential, while  $V_{pl} = 0$ . Knowing  $V(x, y, z)$  and the corresponding electric field, we injected charges with Bohm velocities at locations uniformly distributed on  $S_{sh}$  and computed their trajectories until they reached  $S_e$ . For instance, the cross section of  $V(x = 0, y, z)$  for a square electrode of length  $L = 0.01$  m, insulated on the back side, is presented in Fig. 1(a) together with trajectories of several positive ions entering in the sheath at equidistant locations, where  $V_0 = -300$  V,  $n_i = 10^{15} \text{ m}^{-3}$ ,  $T_e = 2$  eV,  $T_i = 0.2$  eV, and  $n_{ni} = 0$ . Let  $(x_0, y_0, z_0)$  be the coordinates of one ion at the sheath edge and  $(v_{x0}, v_{y0}, v_{z0})$  the velocity components in a narrow layer of acceleration delimited by  $-10 \text{ V} < V < 0$ . Since the sheath also expanded in  $z < 0$  direction, ions entering in the sheath with  $z_0 < 0$  [trajectories from location (1) to (2)] have initially  $v_{z0} > 0$

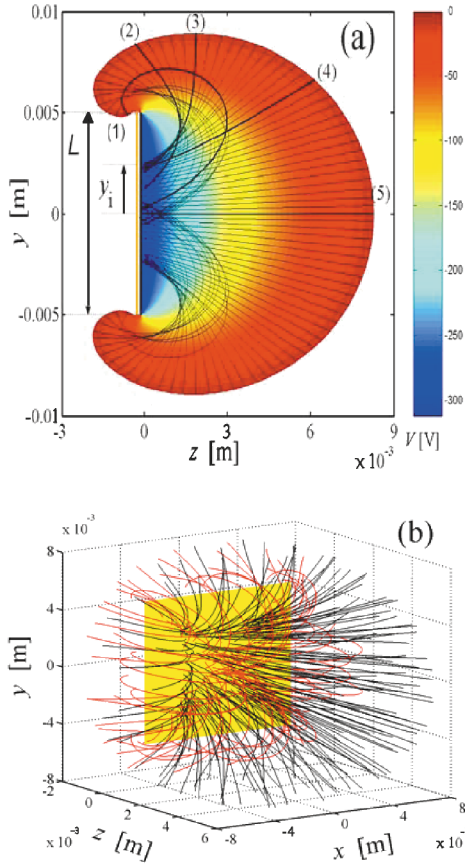


FIG. 1 (color). (a)  $V(x = 0, y, z)$  for a square electrode of length  $L = 0.01$  m, insulated on the back side ( $-z$  direction) including trajectories of several positive ions entering in the sheath at equidistant locations, where  $V_0 = -300$  V,  $n_i = 10^{15}$  m $^{-3}$ ,  $T_e = 2$  eV,  $T_i = 0.2$  eV, and  $n_{ni} = 0$ . (b) Trajectories of 400 ions passing through the sheath where the red lines correspond to ions entering with  $z_0 < 0$  (back side ions) and black for  $z_0 \geq 0$  (frontal ions). The color bar indicates the sheath potential.

to finally reach the central part of  $S_e$  with  $v_z < 0$  at a low incidence angle,  $\alpha_{inc}$  ( $\alpha_{inc} = 90^\circ$  for normal incidence). From (2) to (3),  $v_{z0} \geq 0$  and ions were focused to locations of larger  $|y|$ . From (3) to (4) all positive ions were focused to a very narrow region on  $S_e$  while from (4) to (5) ions exhibited lower velocity components in the  $y$  direction. Thus, this particular kinetics resulted in the formation of PS near the edge,  $y_i \leq |y| \leq L/2$ , an intense focusing ring for  $|y|$  slightly lower than  $y_i$ , and a spotlike structure at the center of AS created by ions entering in the sheath with  $z_0 \leq 0$  ( $y_i$  delimits PS from AS). Trajectories of 400 ions passing through the entire 3D sheath presented as an  $x = 0$  projection in Fig. 1(a) are shown in Fig. 1(b) with red for ions with  $z_0 < 0$  (back side ions) and black for  $z_0 \geq 0$  (frontal ions). For visibility we chose  $-0.002 \leq y \leq 0.006$  mm. The yellow surface corresponds to the electrode. Thus, since a large number of frontal ions form a starlike structure between PS and AS, the back side ions followed complex trajectories.

In order to clarify this kinetic let us divide the entire sheath in quarters delineated by the electrode diagonals.

The impact locations on  $S_e$  of 2000 positive ions entering in sheath from two adjacent quarters are shown in Fig. 2(a) in red ( $AOB$ ) and black ( $BOC$ ), respectively, where dots correspond to frontal ions and open circles to back side ions. While frontal ions were restrictively focused on the area delineated by semidiagonals  $AO$ ,  $OB$ , and the PS with  $\beta = 90^\circ$ , the back side ions reached a larger area delineated by the contour  $AW_2BOA$ . Moreover, frontal ions corresponding to entrance locations from (2) to (4) in Fig. 1(a) were focused to a very narrow region on the surface leading to a starlike profile that sharply delineated the PS from the AS. Because each half of one corner was formed by frontal ions coming from distinct lateral sides of the electrode, one can expect that, at locations indicated with 1 and 2 in Fig. 2(a),  $\alpha_{imp}$  should be symmetric with respect to the diagonal. The back side ions showed some preferential directions such as  $BW_1$ ,  $BW_2$ ,  $CW_1$ , and so on so that one can define the angles  $\alpha_1$  given by  $W_1BW_2$  and  $\alpha_2$  given by  $BW_1C$ . It is important to notice that by sheath expansion,  $W_1$  and  $W_2$  are shifted away from AS eventually reaching the PS. Impact location on the electrode surface of 6000 ions is shown in Fig. 2(b) with different colors for

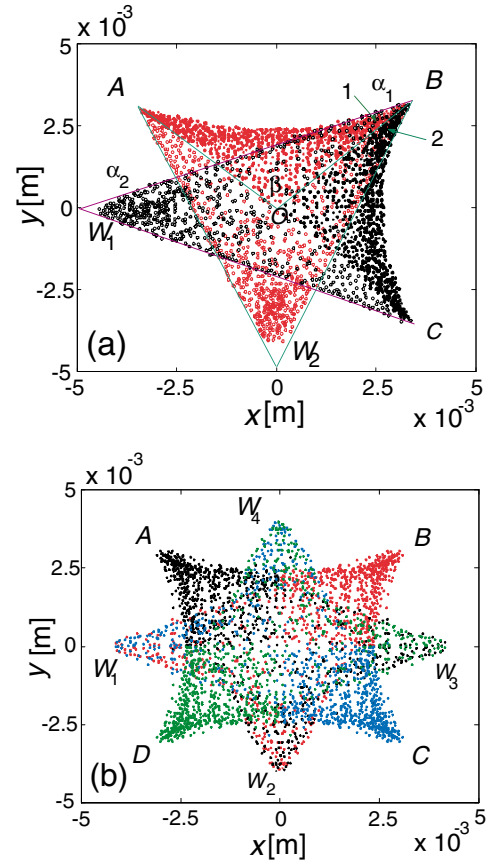


FIG. 2 (color). (a) The impact locations on  $S_e$  of 2000 positive ions entering in sheath from two adjacent quarters where dots correspond to frontal ions and open circles to back side ions. (b) Impact location on the electrode surface of 6000 ions shown with different colors for each corner. For both simulations  $V_0 = -300$  V,  $n_i = 10^{15}$  m $^{-3}$ ,  $T_e = 2$  eV,  $T_i = 0.2$  eV, and  $n_{ni} = 0$ .

each corner delineated by median planes. Thus, the back side ions entering in the sheath from the same corner are diverged in two wings depending from what side of the corner they are originating, eventually forming  $W_1$ ,  $W_2$ ,  $W_3$ , and  $W_4$ . The  $\alpha_1$  and  $\alpha_2$  are dependent on the angle of the electrode corner, and not only on the sheath thickness. Taking into account that line  $BW_2$  in Fig. 2(a) is related to the lateral side  $AB$  and the line  $BW_1$  to the lateral side  $BC$ , then by enlarging the corner angle  $W_1$  and  $W_2$  should get closer to each other, thus reducing  $\alpha_1$ .

Experiments were performed in a dc discharge produced in a cylindrical chamber 35 cm in diameter and 40 cm in length of which outer walls were covered with permanent magnets. Plasma was produced between a filament working as cathode (biased at  $-100$  V) and the grounded anode. The discharge current was adjusted by changing the filament current so that we could set a desired plasma density (usually below  $5 \times 10^{16} \text{ m}^{-3}$ ) by monitoring it with a Langmuir probe which also gives us  $T_e$ ,  $T_{ni}$ , and  $n_{ni}/n_e$  [14]. Ar,  $\text{SF}_6$ , and  $\text{CF}_4$  gases were used to produce electro-positive and electro-negative plasmas (major species  $\text{SF}_6^-$ ,  $\text{SF}_5^-$ , and  $\text{F}^-$ ). Square and octagonal electrodes of 12 mm in diagonal length were made of brass plate, 0.2 mm in thickness, covered on the back side with a thin layer of alumina cement of about 0.5 mm. Because the electrode area is very small with respect to wall area, the shift in plasma potential when applying  $V_0 > V_{pl}$  was less than a few volts. Photographs of square and octagonal electrodes exposed to Ar,  $\text{CF}_4$ , and Ar/ $\text{SF}_6$  plasma are presented in Fig. 3 where electrodes (a) and (d) were treated simultaneously in Ar plasma for 1 h with  $V_0 = -200$  V, electrodes (b) and (e) in  $\text{CF}_4$  plasma ( $n_{ni}/n_e = 4$ ) for 5 min with  $V_0 = 300$  V, and electrodes (c) and (f) in Ar/ $\text{SF}_6$  plasma ( $n_{ni}/n_e = 17$ ) for 5 min with  $V_0 = 200$  V. For all electrodes, the plasma density was kept to  $\cong 10^{15} \text{ m}^{-3}$  and the discharge pressure to 3 mTorr. Thus, in Figs. 3(a) and 3(d) one can see the formation of PS, the intense sputtered ring at the edge of AS, and the appearance of the modal focusing caused by back side ions including distinct lines, named “modal lines” [ $BW_1$ ,  $BW_2$ ,  $CW_1$ , and so on in Fig. 2(a)]. As predicted in Fig. 2(b) locations on PS corresponding from  $W_1$  to  $W_4$  are illustrated in Fig. 3(a) by small arrows. These “modal spots” are also visible (depending on the surface illumination) at some locations in the left-hand side of Fig. 3(d). As previously reported, negative charges follow a similar kinetics within the sheath as positive ions [13]. However, only negative ions can produce significant sputtering, due to heavy mass, while electrons mainly produce thermal effects. As shown in Figs. 3(b), 3(c), 3(e), and 3(f) negative ion bombardment on square and octagonal electrodes reveals a similar modal focusing as that obtained for positive ions. Because of a significantly shorter time of exposure, the visualization of PS and AS, and the formation of the modal lines, is a combined result of sputtering by negative ions, deposition of S, F, or C compounds, and thermal effects by electron

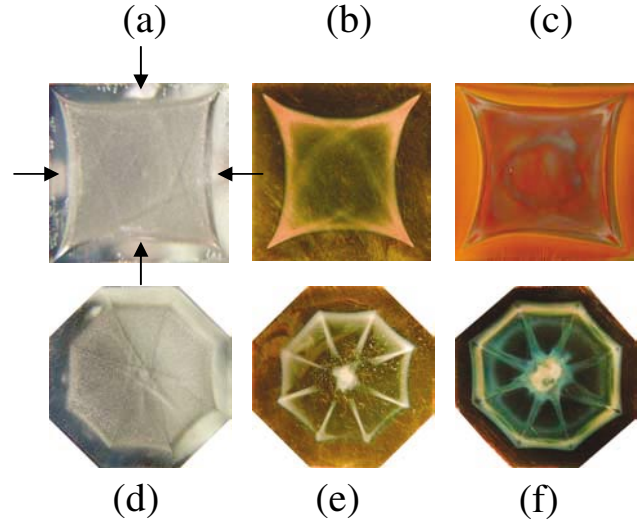


FIG. 3 (color). Photographs of square and octagonal electrodes exposed to Ar,  $\text{CF}_4$ , and Ar/ $\text{SF}_6$  plasmas. (a) and (d) were treated simultaneously in Ar plasma for 1 h with  $V_0 = -200$  V; (b) and (e) in  $\text{CF}_4$  plasma ( $n_{ni}/n_e = 4$ ) for 5 min with  $V_0 = 300$  V; (c) and (f) in Ar/ $\text{SF}_6$  plasma ( $n_{ni}/n_e = 17$ ) for 5 min with  $V_0 = 200$  V. For all electrodes the plasma density was kept to  $\cong 10^{15} \text{ m}^{-3}$  and the discharge pressure to 3 mTorr.

bombardment. No modal spots were observed in the case of negative ion focusing beside a central spot resulted by merging of modal lines. When the electrodes were exposed for a longer time, heating by electron bombardment induced some damage in the focusing pattern starting from the center as can be seen in Fig. 3(f).

If the modal focusing is produced by back side ions, then their absence should lead to the absence of modal lines. Such an example is shown in Fig. 4(a) where the photograph of an octagonal electrode (of 12 mm in circum-radius) having an insulating disk of 25 mm in diameter in the plane of  $z = 0$  and treated in Ar plasma for 1 h is presented, where  $V_0 = -300$  V,  $n_e = 10^{15} \text{ m}^{-3}$ , and  $T_e = 1.7$  eV. The PS still preserves the traces from polishing (no ion impact) while the definition of the edge separating the PS from AS is very sharp. Significant sputtering took place at the edge of AS while its central part does not show any traces of modal lines proving their link to the back side ions which are not present in this case. The impact locations of 5000 negative ions on the surface of an octagonal planar electrode with the back side set as insulator are presented in Fig. 4(b) with red for back side ions and black for frontal ions, where  $n_i = 10^{15} \text{ m}^{-3}$ ,  $V_0 = 200$  V,  $V_{sh} = 1$  V,  $T_e = 2$  eV,  $T_i = T_{ni} = 0.2$  eV, and  $n_{ni}/n_e = 5$ . The frontal ions were mainly focused to an octagonal starlike profile similar to that observed experimentally in Figs. 3(d)–3(f) and Fig. 4(a), while the back side ions clearly show the formation of modal lines with a lower  $\alpha_1$  as a result of increasing the corner angle. The formation of the spotlike focusing at the electrode center is due to the merging of structures such as from  $W_1$  to  $W_4$  in Fig. 2(b). When the simulation was done

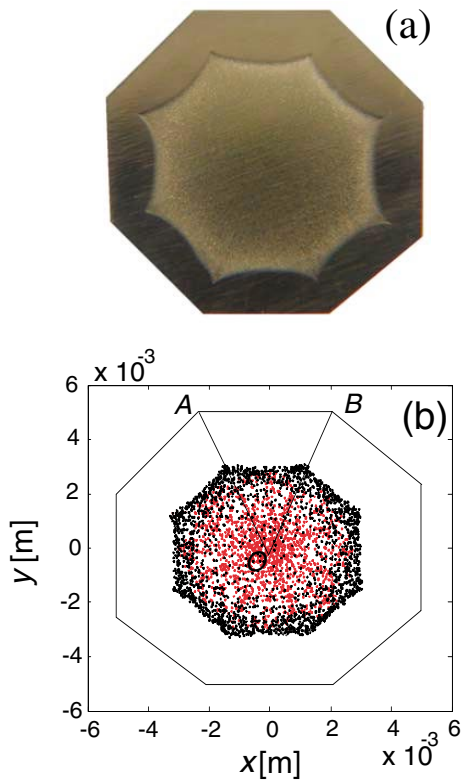


FIG. 4 (color). (a) Photograph of an octagonal electrode (of 12 mm in circumradius) having an insulating disk of 25 mm in diameter in the plane of  $z = 0$  and treated in Ar plasma for 1 h, where  $V_0 = -300$  V,  $n_e = 10^{15}$  m $^{-3}$ , and  $T_e = 1.7$  eV. (b) The impact locations of 5000 negative ions on the surface of an octagonal planar electrode with the back side set as insulator. Red dots correspond to back side ions and black dots to frontal ions ( $n_i = 10^{15}$  m $^{-3}$ ,  $V_0 = 200$  V,  $T_e = 2$  eV,  $T_i = T_{ni} = 0.2$  eV, and  $n_{ni}/n_e = 5$ ).

including an insulator that surrounded the electrode in the plane  $z = 0$  we obtained a similar result as that presented in Fig. 4(b) except for the presence of the red dots, thus resembling exactly the experimental result from Fig. 4(a).

In order to prove that ions that form a corner are impinging the surface coming from distinct lateral sides of the electrode, we took two SEM images to the square presented in Fig. 3(a) at locations similar with (1) and (2) in Fig. 2(a). The electrode was not rotated during investigation. As can be seen from Fig. 5(a), the surface morphology after sputtering by positive ions clearly demonstrates that  $\alpha_{\text{imp}}$  was symmetrically disposed with respect to diagonals. For consistency, the surface morphology at similar locations but on the opposite corner is presented in Fig. 5(c) and 5(d).

In conclusion, we demonstrated for the first time, by simulations and experiments, the existence of a modal focusing effect of positive and negative ions passing through the sheath evolving to finite electrodes immersed

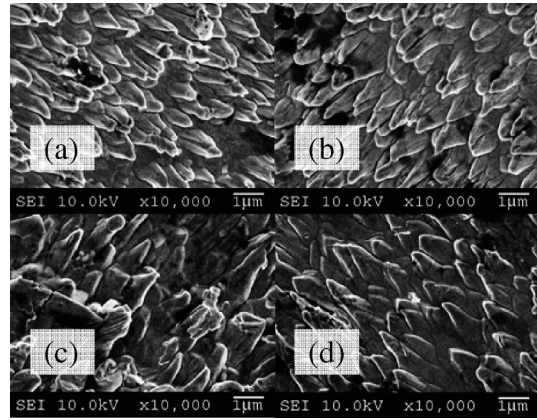


FIG. 5. (a), (b) Surface morphology by SEM of the sample presented in Fig. 3(a) at locations similar to (1) and (2) in Fig. 2(a); (c) and (d) represent similar locations on the opposite corner.

in plasma. The effect consists of the appearance of modal lines and modal spots on the surface of biased electrodes that interface insulators. The superposition of this phenomenon to the already demonstrated discrete-focusing effect significantly increases the complexity of the ion flux on the electrode surface. Present results are expected to have a significant importance to future investigations of finite plasma-sheath structures.

This work was partially supported by the 21st Century Center of Excellence Program of the Ministry of Education, Culture, Sports, Science, and Technology, Japan.

- 
- [1] I. Langmuir, Phys. Rev. **33**, 954 (1929).
  - [2] V. Godyak and N. Stemberg, Phys. Plasmas **9**, 4427 (2002).
  - [3] R.N. Franklin and J. Snell, Phys. Plasmas **8**, 643 (2001).
  - [4] K.-U. Riemann and L. Tsendin, J. Appl. Phys. **90**, 5487 (2001).
  - [5] V. Vahedi, R. A. Stewart, and M. A. Lieberman, J. Vac. Sci. Technol. A **11**, 1275 (1993).
  - [6] A. Kono, Phys. Plasmas **10**, 4181 (2003).
  - [7] R. A. Gottscho, Phys. Rev. A **36**, 2233 (1987).
  - [8] I. J. Donnelly and P. A. Watterson, J. Phys. D **22**, 90 (1989).
  - [9] T. E. Seridan, Appl. Phys. Lett. **68**, 1918 (1996).
  - [10] D. Kim and D. J. Economou, J. Appl. Phys. **94**, 2852 (2003).
  - [11] E. V. Barnat and G. A. Hebner, Appl. Phys. Lett. **85**, 3393 (2004).
  - [12] E. Stamate and K. Ohe, Appl. Phys. Lett. **78**, 153 (2001).
  - [13] E. Stamate, H. Sugai, O. Takai, and K. Ohe, J. Appl. Phys. **95**, 830 (2004).
  - [14] E. Stamate and K. Ohe, J. Appl. Phys. **84**, 2450 (1998).